

論文 著書情報  
Article Book Information

Title	Drained monotonic responses of suffusionless soils
Authors	Lin Ke, Akhio Takahashi
Citation	Journal of Geotechnical and Geoenvironmental Engineering, Vol. 141, Issue 8, 4015033
Pub. date	2015/8
Copyright	© 2015 American Society of Civil Engineers
Note	This material may be downloaded for personal use only. Any other use requires prior permission of the American Society of Civil Engineers. This material may be found at <a href="http://dx.doi.org/10.1061/(ASCE)GT/1943-5606(2015)1327">http://dx.doi.org/10.1061/(ASCE)GT/1943-5606(2015)1327</a>
Note	This file is author's final version.

1 **Drained monotonic responses of suffusional cohesionless soils**

2  
3 **Lin Ke<sup>1</sup> and Akihiro Takahashi<sup>2</sup>**

4  
5 **Abstract**

6  
7 Mechanical consequences of suffusion on the non-cohesive soils with various initial fines  
8 contents under different initial effective confining pressures are presented in this paper. By  
9 use of the modified triaxial permeameter, seepage tests and successive drained monotonic  
10 compression tests are performed. It is found that soil drained strength decreases after  
11 suffusion and a temporary drop in stiffness at the initial stage of shearing with respect to the  
12 axial strain ranging from 0% ~ 1% is observed. The tests suggest that suffusion might create a  
13 distinct packing of soil grains, which might result from possible accumulation of fine grains  
14 at the spots where the constriction size, representing the size of pore channels in a soil, is  
15 smaller than that of fines. Those “surviving” fines after suffusion may function as  
16 reinforcement or jamming at the subsequent compression, resulting in a larger initial stiffness  
17 of the suffusional soils.

18 **Keywords:** suffusion; drained response; cohesionless soil; soil packing

19  
20 **Journal of Geotechnical and Geoenvironmental Engineering, 141(8), 04015033, 2015**

21 **Original URL:**

22 [http://dx.doi.org/10.1061/\(ASCE\)GT.1943-5606.0001327](http://dx.doi.org/10.1061/(ASCE)GT.1943-5606.0001327)

23  

---

<sup>1</sup> Postdoctoral Researcher, Department of Civil Engineering, Tokyo Institute of Technology, 2-12-1 Ookayama, Meguro, Tokyo 152-8552, Japan. E-mail: tsingtaolin@gmail.com

<sup>2</sup> Professor, Department of Civil Engineering, Tokyo Institute of Technology, 2-12-1 Ookayama, Meguro, Tokyo 152-8552, Japan (corresponding author). E-mail: takihiro@cv.titech.ac.jp

## 24 **Introduction**

25

26 The phenomenon of suffusion in cohesionless soils exhibits itself as the gradual migration of  
27 fine grains through the voids of the coarse matrix, transported by volumes of seepage water.  
28 It is frequently detected in natural deposit and in earthen structures. The chronic process of  
29 suffusion always accompanies with the significant dislodgement of soil grains and changes in  
30 hydraulic conductivity. Suffusion may result in a loose soil structure because of the loss of  
31 fine grains without great changes in the voids of the coarse matrix. The stress ~ strain  
32 relationship of the suffusional soil might be greatly altered compared with the soil without  
33 suffusion. There is a high possibility that the strength of the post-suffusion soil decreases due  
34 to the destructive function of suffusion. Sugita *et al.* (2008) reported flow slide of several  
35 embankments constructed on catchment topography (i.e., swamps and valleys) during Noto  
36 Peninsula Earthquake of Japan. Because of the ground configuration, those embankments  
37 may have been suffering from years of suffusion and chronically become too weak to resist  
38 seismic shakings.

39

40 Although soil suffusion might be a huge threat for the stability of existing earthen structures,  
41 unfortunately, few studies could comprehensively investigate the consequences of soil  
42 suffusion from the perspective of soil mechanics. Chang and Zhang (2011) conducted drained  
43 monotonic compression tests on a series of suffusional soil specimens in a revised triaxial  
44 apparatus at different stress states. They concluded that the originally dilative soil would  
45 become contractive after the loss of significant amounts of fine grains and the drained  
46 strength decreased after the suffusion. Undrained monotonic compression tests on internally  
47 eroded soil have been performed by Xiao and Shwiyhat (2012). They illustrated that the peak  
48 deviator stress of suffusional soil was larger than that of the soil without suffusion, which

49 may be attributed to the low degree of saturation. Chang and Meidani (2012) classified the  
50 mechanical behavior of suffusional soil into two categories depending on the confining  
51 pressure when suffusion occurs. For the soil specimens that suffered suffusion under low  
52 confining pressure, the post-suffusion void ratio was on the dense side of the steady state line  
53 in void ratio  $\sim$  mean effective stress space, indicating a dilative response, whereas those  
54 specimens that experienced suffusion under large confining pressure showed much  
55 contractive response with a lower undrained strength. The mechanical consequences of  
56 suffusion on soil seem to be obscure, which probably is due to the low saturation degree of  
57 the tested specimens after suffusion. Xiao and Shwiyhat (2012) noted that the B-value of the  
58 eroded soil specimens immediately after suffusion was approximately 0.86. The complicated  
59 unsaturated soil behavior may produce confusing results. Therefore, further detailed testing  
60 with the accurate measurements of pressures is necessary to elaborate the mechanical  
61 behavior of eroded soil. Meanwhile, models for assessing the mechanical consequences of  
62 suffusion have been proposed by Muir Wood *et al.* (2010). In their approach, the progress of  
63 suffusion was approximated by progressively removing of grains from the assemblies of  
64 circular discs at different stages of shearing. The modelling indicated that the suffusion would  
65 alter the soil state from “dense” to “loose”. Hicher (2013) predicted the mechanical behavior  
66 of granular materials subjected to particle removal by a micromechanics-based model and  
67 concluded that erosion of soils may trigger diffuse failure in an earthen structure.

68

69 Full comprehension of the post-suffusion soil behavior is beneficial for the assessment of the  
70 stability of potentially eroded earthen structures, such as levees. This study mainly discusses  
71 the mechanical consequences of suffusion on non-cohesive soils. By utilizing the modified  
72 triaxial permeameter, drained monotonic compression tests are performed on the suffusional  
73 specimens, which would be helpful to understand the mechanical characteristics of

74 suffusional cohesionless soil.

75

## 76 **Experimental investigations**

77

78 The experimental investigations are performed using a modified triaxial permeameter, which  
79 is capable of directly investigating not only the mechanism of suffusion but also the  
80 corresponding change of soil mechanical behaviors induced by erosion of fine grains.  
81 Detailed descriptions of the permeameter could be referred to Ke and Takahashi (2014).

82

### 83 ***Test materials***

84 In this study, the tested sand includes two types of silica sand (Silica No.3 and No.8) with the  
85 same specific gravity of 2.645 but different dominant grain sizes (Ke and Takahashi 2012).  
86 They are commercially available sands, frequently used as industrial polishing materials. The  
87 siliceous sand is mainly composed by quartz, categorized as sub-rounded to sub-angular  
88 material. Before testing, they are fully washed and dried to remove impurities. The grain size  
89 distributions of Silica No.3 and No.8 are plotted in Fig. 1. Silica No.3 and No.8 correspond to  
90 medium sand and fine sand, respectively (ASTM D2487-11). With larger grain size, Silica  
91 No.3 works as the coarse fractions which are regarded as soil skeleton in the mixture,  
92 whereas Silica No.8 is the erodible fine grains. Hereafter, without specification, the term  
93 “fine grains” is referred to Silica No.8 for simplicity. The tested specimens are the binary  
94 mixtures of the two sands by three different fines contents (percentage of mass ratios of fine  
95 grains to total weight of soil specimen, *FC*), which are 35%, 25% and 15%. The grain size  
96 distributions of the mixtures are shown in Fig. 1 indicating that all of the three specimens are  
97 gap-graded. The vulnerability of tested specimens to suffusion are assessed by Kezdi’s  
98 method (Kezdi, 1979), which indicates internally unstable characteristic of tested soils

99  $((D_{15c}/d_{85f})_{\text{gap}}=7.9>4$ , where  $D_{15c}$  is the particle size at 15% by passing is finer of Silica No.3  
100 (mm) and  $d_{85f}$  refers to the particle size at 85% by passing is finer of Silica No.8 (mm)).  
101 Maximum and Minimum void ratios ( $e_{\text{max}}$  and  $e_{\text{min}}$ ) of tested soil are summarized in Table 1,  
102 showing that an increasing in the fines content results in a proportional reduction of  $e_{\text{max}}$  and  
103  $e_{\text{min}}$  within 0~35% fines content. This type of binary mixture is commonly referred as “coarse  
104 domain soil” and the mechanical responses are largely dependent on the coarse fractions  
105 (Lade *et al.*, 1998; Cubrinovski and Ishihara, 2002).

106

107 A summary of the test cases is shown in Table 2, where initial void ratio refers to the void  
108 ratio of tested specimens under an effective confining pressure of 20kPa prior to  
109 consolidation. Each specimen is prepared by moist tamping method that soil mixtures with an  
110 initial moisture content of 10% are tamped to the target void ratio to avoid the segregation of  
111 the two kinds of grains with different dominant sizes. A non-linear average undercompaction  
112 criterion (Jiang *et al.*, 2003) is adopted to generate uniform soil specimens. The tamping on  
113 each specimen is in a systematic manner to guarantee an identical input energy. The mean  
114 effective stress at consolidation considered in this paper is 50kPa, 100kPa and 200kPa, which  
115 approximately corresponds to the vertical effective stress at 5m, 10m and 20m depth,  
116 respectively, on condition that groundwater table is at the ground surface and soil ground is  
117 fully saturated. Some of the specimens experience suffusion at a constant inflow rate of  
118  $5.17 \times 10^{-6} \text{m}^3/\text{s}$  in the modified triaxial cell.

119

### 120 ***Test program***

121 The initial diameter and height of the moist tamped specimens prior to saturation is  
122 approximately 70mm and 150mm, respectively. Necessary corrections, such as the effects of  
123 buoyancy of the cap and soil, and membrane stiffness, have been considered. Overall, the test

124 program includes soil preparation, vacuum saturation, consolidation, seepage test and  
125 compression test. A schematic diagram of the test procedure in the  $p'$ - $q$  stress space (mean  
126 effective stress ~ deviator stress) is presented in Fig. 2. Vacuum saturation procedure (ASTM  
127 D4767-11) is utilized to saturate the soil specimens. Approximately, the deaerated water with  
128 a volume of 10.4 (normalized value in terms of pore volume) has been flowed through the  
129 soil specimen. For the majority of tests, B values of at least 0.95 could be achieved after the  
130 applying of 100kPa back pressure following the vacuum saturation procedure. The axial  
131 displacement and average radial displacement have been recorded all the way to update the  
132 present dimension of tested specimens. Upon completion of saturation, soil specimens are  
133 isotropically consolidated until the preferred mean effective stress (i.e., 50kPa, 100kPa or  
134 200kPa in this study) is reached. Seepage tests are performed at the stress state the same as  
135 that of the specimen after isotropic consolidation. To demonstrate the mechanical effects of  
136 suffusion on soils systematically, the imposed inflow rate for each specimen keeps constant  
137 as  $5.17 \times 10^{-6} \text{m}^3/\text{s}$ , which is determined by considering the requirement of laminar flow,  
138 restriction of excess hydrostatic pressure and acceptable range of fines loss. It may be argued  
139 that a constant inflow rate could not reflect the real hydraulic conditions in dams, which is a  
140 limitation of the apparatus. The seepage tests would be terminated at least after 3 hours. At  
141 most circumstances, the post-suffusion B-value is larger than 0.93 because of the  
142 maintenance of back pressure on the tested specimens. The axial displacement, radial  
143 deformation and cumulative eroded fines mass are recorded to determine the fines content  
144 and post-suffusion void ratio, which are of significance for the assessment of mechanical  
145 responses. After the seepage test, a series of monotonic compression test is performed on the  
146 suffusional soil without changing the cell pressure and the back pressure to investigate the  
147 mechanical consequences of suffusion. The compression test, either drained or undrained test,  
148 is displacement controlled with an axial strain rate of 0.1%/min, following the standard

149 criteria (ASTM D4767-11; ASTM D7181-11). The cell pressure is maintained constant while  
150 the specimens are compressed at the designated strain rate.

151

### 152 **Mechanical influences of Silica No.8**

153

154 It is universally recognized that the presence of nonplastic fines creates a “metastable” soil  
155 structure, which fundamentally alters the soil mechanical response at shearing from that of  
156 clean sand. However, regarding the mechanical function of those nonplastic fines debates still  
157 exist. In this paper, the tested soil mixtures contain amounts of nonplastic fine grains, Silica  
158 No.8, up to 35% in mass ratio. The mechanical effects of Silica No.8 are elaborated first and  
159 further mechanical behavior of soil before and after suffusion could be compared directly.

160

161 Figure 3 plots the relations of axial strain and deviator stress, and the corresponding effective  
162 stress paths in  $p'$ - $q$  diagram of the specimens with the fines contents of 35%, 25%, 15% and  
163 0%, respectively, under an initial effective confining pressure of 50kPa, in the triaxial  
164 compression tests under undrained condition. The skeleton sand consists of the coarse Silica  
165 No.3 sand, whereas Silica No.8 serves as nonplastic fine grains. The reconstituted specimens  
166 with fine grains are prepared by moist tamping method with an initial relative density of  
167 approximate 47%. The moist tamped specimen of Silica No.3 is targeted at the largest  
168 achievable void ratio to accentuate its dilative tendency even at loose condition. Details of  
169 those specimens have been listed in Table 2. It is obviously noted that the presence of Silica  
170 No.8 would decrease the soil strength, which may be attributed to the lubrication between  
171 skeleton grains by the nonplastic fine grains, thereby smoothing the contacts among the  
172 coarse grains. The loss of effective contacts may result in smaller soil stiffness and larger  
173 compressibility. Thevanayagam and Mohan (2000) and Thevanayagam (2007) noted similar



174 evidences of the existence of the lubricated soil structures. In terms of effective stress paths,  
175 the specimen with 35% fines content displays fully contractive behavior, whereas the soil  
176 with less fines content becomes more dilative. Loose though, Silica No.3 without fine grains  
177 exhibits fully dilative behavior throughout the compression. It is possible that for the  
178 specimen containing 35% fine grains the coarse grains are separated apart by the relatively  
179 large amounts of loose fine grains and the contractive behavior may be determined by the  
180 compressibility of the fine grains deposited between the coarse grains. With the declining of  
181 fines content, the coarse grains gradually contact with each other. The compression may force  
182 the fine grains to slide into the voids and correspondingly the coarse grains move into a better  
183 contact, causing dilatancy at larger axial strain. In sum, the presence of Silica No.8 decreases  
184 the soil strength and inhibits the dilatancy tendency.

185

## 186 **Test results and discussions**

187

### 188 *Summary of seepage test results*

189 A concise summary of the seepage test results is presented for a fundamental understanding  
190 of suffusion mechanism and its influence on the soil state. The seepage tests are performed by  
191 assigning seepage fluid at a constant rate downwardly through the tested specimens by a flow  
192 pump. The flow velocity, defined as the flow volume passing through unit area in unit time, is  
193 sufficiently slow in the tests to guarantee a laminar flow condition. In the tests, the flow  
194 velocity is gradually increased until it reaches the prescribed value of  $5.17 \times 10^{-6} \text{ m}^3/\text{s}$ . Before  
195 the onset of suffusion, without any fine grains loss, the hydraulic gradient keeps stable. Once  
196 the Darcy velocity reaches critical velocity, the dislodgement of fine grains initiates and  
197 correspondingly hydraulic gradient would drop, resulting in an increase in hydraulic  
198 conductivity. Successive rising of Darcy velocity may further accelerate the progress of

199 suffusion and correspondingly, large amounts of fine grains would be dislodged, resulting in  
200 the contractive deformation of the tested specimens. If the imposed flow rate is kept constant  
201 at a value larger than critical velocity for a long period, the loss of fine grains would  
202 gradually become constant, indicating the gradual decreasing of erosion rate. Along with the  
203 loss of fine grains, coarse fractions may re-arrange their inter-position to reach a new  
204 equilibrium and the volumetric deformation will cease. As a result, the tested specimens will  
205 become loose. A summary of the changes of hydraulic parameters is indicated in Table 3.

206

207 The suffusional behavior of tested specimens is closely dependent on the hydraulic conditions.  
208 In authors' tests, the assignment of seepage flow is realized by gradually raising the inflow  
209 rate up to  $5.17 \times 10^{-6} \text{ m}^3/\text{s}$  and maintaining this rate till several indicators become stable, such  
210 as hydraulic gradient, cumulative eroded soil mass and volumetric strain. Evolution of  
211 percentage of cumulative fines loss with time under different initial effective confining  
212 pressures and initial fines contents is summarized in Figs. 4 and 5, respectively. It is noted  
213 that for each case at the constant imposed flow rate soil experiences an initially sharp loss of  
214 fine grains and gradual decreasing of erosion rate with time. The cumulative eroded soil mass  
215 is larger under the smaller initial effective confining pressure and is larger for the specimens  
216 with the larger initial fines content within the test range. The changes in fines content and  
217 void ratios are summarized in Table 3, where the intergranular void ratio is derived by  
218 regarding the volume of fine grains as that of voids. It is indicated that with the significant  
219 loss of fine grains, the post-suffusion void ratios of tested specimens greatly increase.  
220 Although different in the fines loss and post-suffusion void ratio, the suffusional specimens  
221 with an initial fines content of 35% show similar intergranular void ratios, averagely equaling  
222 to 1.3, which might be a practical comparison base for interpreting the suffusional soil  
223 behavior for this study. The evolution of soil state induced by suffusion is plotted in void ratio

224 ~ fines content space (Fig. 6). The post-suffusion specimens have significantly large void  
225 ratio, even larger than the maximum void ratio, and thus an extremely loose soil packing is  
226 expected. A larger fines content and a smaller void ratio is observed for the specimens on  
227 which seepage tests are performed under larger initial effective confining pressure, compared  
228 with the specimens under lower initial effective confining pressure. Thevanayagam and  
229 Mohan (2000) divided the mechanical behavior of the “coarse domain” soil mixture by a  
230 demarcation line corresponding to  $e_s \approx e_{cmax}$  (maximum void ratio of the coarse fractions) (Fig.  
231 6). The positions of tested specimens are all above the demarcation line, indicating that the  
232 packing of coarse grains is unstable and separated by fine grains, and the soil behavior is  
233 affected by those active fine grains participating in the force chains. Due to the characteristics  
234 of suffusion, local clogging or accumulation of fine grains might occur and consequently, a  
235 particular packing of soil grains might be formed. Therefore, the drained responses of  
236 suffusional soils may be different from that of the soil before suffusion.

237

### 238 ***Influence of initial effective confining pressure on mechanical response of suffusional soil***

239 As is discussed above, a lower effective confining pressure during suffusion would result in  
240 larger volumes of voids in soil and more fines loss, and consequently, the mechanical  
241 behavior of suffusional soil may be closely related with the confining pressure when  
242 suffusion occurs. To reveal this relation, three drained compression tests have been conducted  
243 on the suffusional specimens that initially contain 35% fine grains and have suffered  
244 suffusion under the same initial effective confining pressure of 50kPa, 100kPa and 200kPa,  
245 respectively. Although the post-suffusion void ratios vary for different specimens, the  
246 intergranular void ratios are basically equal (i.e., approximately 1.3). If the intergranular void  
247 ratio is accepted as the effective reference for the comparison of the mechanical behavior of  
248 suffusional soils, the differences in the drained response may be mainly caused by the initial

249 effective confining pressure and the corresponding particular post-suffusion packing of soil  
250 grains. The relation curves of deviator stress and axial strain accompanied with the evolution  
251 of volumetric strain are plotted in Fig. 7, respectively, which indicate a typical contractant  
252 volumetric behavior of loose sand. The deviator stress gradually develops and maintains  
253 constant at a peak value, whereas the contractive volumetric strain rises to maximum and  
254 keep constant. A majority of experimental investigations has revealed that an axial strain of  
255 30% ~ 40% is necessary for achieving critical state of sand in drained test. Unfortunately, the  
256 tests in this study were terminated at the axial strain of about 13% ~ 17%, which should not  
257 be sufficiently large to present the full drained responses of suffusional specimens. To  
258 compensate the limitation of insufficient straining and depict the whole picture of drained  
259 behavior, a hyperbolic curve fitting is adopted to approximate the contractant soil behavior at  
260 drained condition (Ferreira and Bica, 2006) and the extrapolated curves up to an axial strain  
261 of 40% are shown in Fig. 7 by dash lines. It is worth to mention that the dash lines derived  
262 from hyperbolic curve fitting are hypothetical. But considering the significantly large initial  
263 void ratio of suffusional specimens, the fitting may reflect the drained behavior appropriately.  
264 For comparison purpose, results of drained tests on the companion specimens (35N-50, 35N-  
265 100 and 35N-200) under the same stress state as that of suffusional soil are plotted in Fig. 8.  
266 The intergranular void ratio of companion specimens is around 1.4, slightly larger than that of  
267 the suffusional soil. Herein, failure is defined as the soil state wherein the deviator stress  
268 obtained at an axial strain of 15% (ASTM D4767-11; ASTM D7181-11) and correspondingly,  
269 the soil strength refers to the deviator stress at an axial strain of 15%. Figure 9 displays the  
270 stress ratio at failure, ratio of deviator stress to current mean effective stress, against the  
271 initial effective confining pressure, indicating that the soil strength decreases after suffusion  
272 and the extent of decreasing becomes smaller at larger initial effective confining pressure. It  
273 can be explained that under larger initial effective confining pressure, less fine grains would

274 be dislodged by seepage flow and consequently less changes occurred in the packing of soil  
275 grains, resulting in less drop in soil strength after suffusion. In terms of the volumetric strain  
276 at failure in Fig. 10, the patterns of behavior of companion specimens are in accordance with  
277 the common sense: because of the dilatancy tendency soil commonly fails at smaller  
278 volumetric strain under smaller effective confining pressures, and the greater contractive  
279 behavior is expected under larger effective confining pressures. However, a different  
280 response, departing from common sense, is observed for the suffusional specimen: volumetric  
281 strain at failure is larger under lower initial effective confining pressure and it becomes  
282 smaller under larger initial effective confining pressure. It can be understood that under lower  
283 initial effective confining pressure, more fine grains are eroded away and greater increment in  
284 void ratio occurs, and correspondingly at the subsequent compression, for specimen 35E-50,  
285 the effect of void ratio increment may surpass that of the dilatancy tendency under lower  
286 effective confining pressure. Consequently, larger volumetric strain at failure is observed at  
287 low initial effective confining pressure.

288

289 To fully interpret the reduction of soil strength after suffusion, the critical friction angle is  
290 estimated. In this study, the critical state might not be reached at an axial strain of 13% ~ 17%  
291 where compression tests are terminated and extrapolation of the data is necessary. The  
292 identification of critical state is fulfilled by plotting the stress ~ dilatancy relation of the  
293 drained tests on suffusional and companion specimens, and extending the curve to the point  
294 of intersection with the zero dilatancy axis. An unique critical stress ratio  $(q/p')_{cs}$  could be  
295 evaluated as 1.64 and 1.74 for the suffusional and the companion specimens, and accordingly,  
296 the derived critical friction angle is  $40.1^\circ$  and  $42.4^\circ$ , respectively. Due to suffusion, the  
297 critical friction angle decreases by 5.7%. It may be argued that as an intrinsic physical  
298 property critical friction angle should be constant regardless of the change of void ratio after

299 suffusion. However, accompanying with void ratio variation, fines content of suffusional  
300 specimens have been significantly reduced, which may cause the reduction of critical friction  
301 angle. Further experimental investigations on relative angularity of tested grains might be  
302 beneficial to explain the change of friction angle, which might beyond the scope of the study.  
303

304 Besides, a temporary declining in soil stiffness at the initial stage of shearing with respect to  
305 the axial strain ranging from 0% ~ 1% is observed. Figure 11 displays the variation of secant  
306 stiffness at the initial 1% of axial strain. The soil stiffness has been normalized by the current  
307 mean effective stress in order to compare the cases with different effective confining  
308 pressures and accentuate the uniqueness of suffusion induced packing of soil grains. For the  
309 comparison purpose, the secant stiffness of the companion specimens is superimposed. Since  
310 the companion specimens are similar in terms of the initial fines content and void ratio, the  
311 variation of normalized secant stiffness with axial strain displays identical patterns of  
312 behavior. The stiffness shows the initially largest value and declines with further compression.  
313 However, the behavior pattern of the suffusional specimens is distinct from the companion  
314 specimens in three aspects. Firstly, the initial secant stiffness becomes larger than that of the  
315 companion specimens, which may be explained by the reinforced soil packing created by  
316 suffusion. It is postulated that fine grains may probably be impeded and gradually accumulate  
317 at the spots where the size of the pore tunnels, formed by coarse grains, is less than that of the  
318 fine grains. At subsequent compression, those fine grains function as jamming rather than  
319 lubrication, and thereby reinforcing the packing of soil grains. Secondly, temporary drops in  
320 soil stiffness are observed for suffusional specimens 35E-50, 35E-100 and 35E-200, at the  
321 axial strain of 0.5%, 0.4% and 0.2%, respectively. It is considered as the evidence of the  
322 deterioration of the temporary reinforced soil packing with further straining. Under larger  
323 effective confining pressure, the reinforcement may be easily destroyed and therefore, the

324 stiffness drop in specimen 35E-200 is found at lower axial strain. Thirdly, because of the  
325 extremely loose state of the suffusional specimens, the normalized secant stiffness keeps  
326 lower than that of the companion specimens after the stiffness drop.

327

### 328 *Influence of initial fines content on mechanical response of suffusional soil*

329 Differences in initial fines content directly result in a different soil packing before suffusion,  
330 which will exert an influence on the progress of suffusion and the post-suffusion soil packing.

331 As is shown in Fig. 5, a larger amount of fines loss is observed at the specimen with larger  
332 initial fines content. An understanding of the effects of initial fines content may shed light on  
333 the evolution of soil packing during suffusion and mechanical responses of suffusional soil.

334 The analysis below is limited to the tests under an initial effective confining pressure of  
335 50kPa, which show the largest increment in void ratio and drop in soil strength.

336

337 In a specimen, a fraction of fine grains fill the voids, whereas another fine grains separate the  
338 coarse grains. Since the fine grains occupying the voids among the coarse grains may hardly  
339 participate in force chains (Skempton and Brogan, 1994), the fine grains in the voids may be  
340 vulnerable to suffusion and probably dislodged by seepage flow. Erosion of the fine grains  
341 effectively separating the coarse grains may occur at larger Darcy's flow and the  
342 rearrangement of coarse grains occurs to reach new equilibrium. Majority of the "surviving"  
343 fine grains after three-hour seepage test are wedged between coarse grains and actively  
344 participating in the force chains. Because of the larger voids size among coarse grains of the  
345 specimen with 35% initial fines content (specimen 35E-50) compared with other specimens  
346 (specimen 25E-50 and 15E-50), if the relative density is similar and fine grains are merely  
347 considered as voids, specimen 35E-50 may show larger loss of fine grains. Under the same  
348 initial effective confining pressure of 50kPa, different although the initial fines content is, the

349 specimens show approximately similar post-suffusion fines content (i.e., 10%~13%) but  
350 different post-suffusion void ratios, as is shown in Table 3. Because of the obvious  
351 differences in post-suffusion void ratio, the drained responses of those suffusional specimens  
352 should be different. Figure 12 shows the results of drained compression test on specimen  
353 35E-50, 25E-50 and 15E-50 under an initial effective confining pressure of 50kPa. Specimen  
354 35E-50, which is the largest in post-suffusion void ratio, exhibits the lowest soil strength and  
355 secant stiffness. In terms of volumetric strain, three specimens show similar amounts of  
356 contractive strain within the initial 6% axial strain. Afterwards, specimen 15E-50, which is  
357 the smallest in post-suffusion void ratio, become dilative at an axial strain of 14%, and  
358 similarly specimen 25E-50 exhibiting dilatancy at an axial strain of 19%. Specimen 35E-50  
359 does not show dilative behavior within test range.

360

#### 361 **Distinctive packing of soil grains after suffusion**

362

363 Monotonic compression tests have revealed the somewhat different soil responses of the  
364 suffusional soil: under the larger initial effective confining pressure it exhibits a less  
365 volumetric strain and a temporal decline in soil secant stiffness is observed within the initial  
366 1% axial strain. Since the intergranular void ratio of the suffusional specimens are  
367 approximately the same and the effective confining pressure may not be sufficiently large to  
368 trigger grain crushing (i.e., a maximum initial effective confining pressure of 200kPa), the  
369 soil responses should be dominated by the post-suffusion soil packing and the soil grain  
370 movement during shearing.

371

372 To signify the distinguished packing of soil grains after suffusion, monotonic drained test on  
373 a reconstitute specimen with similar fines content and initial void ratio as that of suffusional



374 specimen 35E-50 is performed. The reconstituted specimen with an initial fines content of  
375 15% is prepared by moist tamping method, targeting at the largest achievable void ratio.  
376 Because of the occurrence of large volumetric deformation during consolidation, the void  
377 ratio before compression is 0.81, still less than the post-suffusion void ratio of 1.0 for  
378 specimen 35E-50. Figure 13 shows the drained responses of the two specimens in terms of  
379 stress ~ strain relationship and corresponding development of volumetric strain. Due to the  
380 larger void ratio, the suffusional specimen mostly gains less strength. However, careful  
381 examination of the stress ~ strain curves within the initial 1% axial strain shows that the  
382 initial secant stiffness of suffusional specimen is larger than that of the reconstituted  
383 specimen and a sudden drop in deviator stress is observed around 0.5% axial strain, after  
384 which soil strength and secant stiffness keep smaller than those of the reconstituted specimen  
385 throughout the test range.

386

387 The above test suggests a distinguished packing of soil grains after suffusion, different from  
388 reconstituted fine-grains-containing sand. Specifically, compared with the denser  
389 reconstituted specimens, the suffusional specimen still becomes much stiffer at the beginning  
390 of shearing. It is inferred that along with the seepage flow amounts of fine grains keep being  
391 dislodged and coarse grains rearrange their positions into a new equilibrium. Because of  
392 possible clogging, fine grains might be accumulated at the spots where the constriction size,  
393 representing the size of pore channels in a soil, is smaller than that of fine grains. Due to the  
394 rearrangement of grains, those accumulated fine grains may actively participate in force  
395 chains. Different from the function of “lubrication”, those “surviving” fine grains after  
396 suffusion would probably perform like reinforcement or jamming. Thereafter, the reinforced  
397 post-suffusion soil packing renders the suffusional specimen much stiffer and less  
398 compressible at the beginning of shearing. With the subsequent compression the

399 reinforcement is deteriorated and the suffusional specimen may behave like typical fine-  
400 grains-containing sand. To further validate this assumption, a microscopic observation of the  
401 post-suffusion packing of soil grains might be necessary.

402

### 403 **Conclusions**

404

405 The mechanical consequences of suffusion on a series of cohesionless soils are presented in  
406 this paper. The tested specimens consist of the binary mixtures of Silica sand No.3 and No.8.  
407 With larger grain size, Silica No.3 works as the soil skeleton, whereas Silica No.8 is the  
408 erodible fine grains. Mechanically, the presence of Silica No.8 would decrease the soil  
409 strength and inhibit the dilatancy tendency of Silica No.3, which may be due to the  
410 lubrication function of the nonplastic Silica No.8 deposited between the skeleton grains. By  
411 utilizing the modified triaxial permeameter, seepage tests are performed on those specimens  
412 to create suffusion condition, and drained monotonic compression tests are performed on the  
413 suffusional specimens to reveal their mechanical behavior.

414

415 Soil strength decreases after suffusion and the amounts of drops become smaller under larger  
416 initial effective confining pressure. Departing from the pattern of behavior of the companion  
417 specimen, the suffusional soil behaves differently: its volumetric strain at compression is  
418 larger under lower initial effective confining pressure and it becomes smaller under larger  
419 initial effective confining pressure. In terms of soil stiffness, the initial secant stiffness of  
420 suffusional soil becomes larger than that of the companion soil and a temporary drop in soil  
421 stiffness at the initial stage of shearing with respect to the axial strain ranging from 0% ~ 1%  
422 is observed. It may be regarded as the evidence of the deterioration of the temporary  
423 reinforced soil packing with further straining and that reinforcement may be easily destroyed

424 under larger initial effective confining pressure.

425

426 Under the same initial effective confining pressure of 50kPa, the specimen with larger initial  
427 fines content shows a larger amount of fine grains loss during the seepage test, resulting in a  
428 larger post-suffusion void ratio. At the subsequent compression, this specimen would exhibit  
429 lower soil strength and secant stiffness.

430

431 Compression test results have revealed the probable existence of a distinctive packing of soil  
432 grains after suffusion. The “surviving” fine grains after suffusion may actively participate in  
433 the force chains, acting like reinforcement. The reinforced post-suffusion soil packing renders  
434 the suffusional specimen much stiffer and less compressible. With the subsequent  
435 compression the reinforcement will be deteriorated and the suffusional specimen may behave  
436 like typical fine-grains-containing sand.

437

#### 438 **Acknowledgement**

439

440 The first author acknowledges the Japanese Government (Monbukagakusho: MEXT)  
441 scholarship support for performing this research. This work was supported by JSPS  
442 KAKENHI Grant Numbers 25420498.

443

#### 444 **References**

445

446 ASTM D2487-11. (2012). “Standard Practice for Classification of Soils for Engineering  
447 Purposes (Unified Soil Classification System).” *Annual Book of ASTM Standards*, Vol.04.08,  
448 ASTM International, West Conshohocken.

449 ASTM D4767-11. (2012). "Standard Test Method for Consolidated Undrained Triaxial  
450 Compression Test for Cohesive Soils." *Annual Book of ASTM Standards*, Vol.04.08, ASTM  
451 International, West Conshohocken.

452 ASTM D7181-11. (2012). "Method for Consolidated Drained Triaxial Compression Test for  
453 Soils." *Annual Book of ASTM Standards*, Vol.04.09, ASTM International, West  
454 Conshohocken.

455 Chang, C.S., and Meidani, M. (2012). "Deformation and failure behavior of soils under  
456 erosion." *Poster of NSF CMMI Engineering Research and Innovation Conference, Boston,*  
457 *MA, USA, CMMI-0928433.*

458 Chang, D.S., and Zhang, L.M. (2011). "A stress-controlled erosion apparatus for studying  
459 internal erosion in soils." *Geotechnical Testing Journal*, 34(6), 579-589.

460 Cubrinovski, M., and Ishihara, K. (2002). "Maximum and minimum void ratio characteristic  
461 of sands." *Soils and Foundations*, 42(6), 65-78.

462 Ferreira, P.M.V., and Bica, A.V.D. (2006). "Problems in identifying the effects of structure  
463 and critical state in a soil with a transitional behaviour." *Géotechnique*, 56(7), 445-454.

464 Hicher, P.-Y. (2013). "Modelling the impact of particle removal on granular material  
465 behavior." *Géotechnique*, 63(2), 118-128.

466 Jiang, M.J., Konrad, J.M., and Leroueil, S. (2003). "An efficient technique for generating  
467 homogeneous specimens for DEM studies." *Computers and Geotechnics*, 30(7), 579-597.

468 Kezdi, A. (1979). *Soil Physics: Selected Topics (Developments in Geotechnical Engineering)*,  
469 Elsevier Science Ltd., Amsterdam, Netherlands.

470 Ke, L., and Takahashi, A. (2012). "Strength reduction of cohesionless soil due to internal  
471 erosion induced by one-dimensional upward seepage flow." *Soils and Foundations*, 52(4),  
472 698-711.

473 Ke, L., and Takahashi, A. (2014). "Triaxial erosion test for evaluation of mechanical  
474 consequences of internal erosion." *Geotechnical Testing Journal*, 37(2), 347-364.

475 Lade, P.V., Liggió, C.D., Jr., and Yamamuro, J.A. (1998). "Effects of non-plastic fines on  
476 minimum and maximum void ratios of sand." *Geotechnical Testing Journal*, 21(4), 336-347.

477 Muir Wood, D., Maeda, K., and Nukudani, E. (2010). "Modeling mechanical consequences  
478 of erosion." *Géotechnique*, 60(6), 447-457.

479 Skempton, A.W., and Brogan, J.M. (1994). "Experiments on piping in sandy gravels."  
480 *Géotechnique*, 44(3), 449-460.

481 Sugita, H., Sasaki, T., and Nakajima, S. (2008). "Damage investigation of road embankment  
482 caused by the 2007 Noto Peninsula, Japan Earthquake." *Public Works Research Institute*  
483 *Report*.

484 Thevanayagam, S., and Mohan, S. (2000). "Intergranular state variables and stress-strain  
485 behavior of silty sands." *Géotechnique*, 50(1), 1-23.

486 Thevanayagam, S. (2007). "Intergrain contact density indices for granular mixes - I :  
487 Framework." *Earthquake Engineering and Engineering Vibration*, 6(2), 123-134.

488 Xiao, M., and Shwiyhat, N. (2012). "Experiment investigation of the effects of suffusion on  
489 physical and geomechanic characteristics of sandy soils." *Geotechnical Testing Journal*,  
490 35(6), 1-11.

491

492 **Table 1** Physical properties of tested soils

Physical properties	Silica No.3	Silica No.8	Mixtures with 35% Silica No.8	Mixtures with 25% Silica No.8	Mixtures with 15% Silica No.8
Fines content ( <i>FC</i> ) (%)	---	---	35	25	15
Maximum void ratio	0.94	1.33	0.74	0.77	0.79
Minimum void ratio	0.65	0.70	0.36	0.37	0.53

493

494 **Table 2** Details of tested specimens

Specimens	Initial <i>FC</i> (%)	Initial void ratio ( $e_i$ )	Mean effective stress at consolidation (kPa)	Post consolidation void ratio ( $e_c$ )	Relative density (%)	Type of compression
35E-50	35.0	0.59	50	0.55	48.5	Drained
35E-100	35.0	0.60	100	0.56	47.5	Drained
35E-200	35.0	0.64	200	0.57	46.2	Drained
25E-50	25.0	0.61	50	0.60	42.8	Drained
15E-50	15.0	0.68	50	0.68	43.1	Drained
35N-50	35.0	0.59	50	0.55	48.5	Drained
35N-100	35.0	0.61	100	0.56	47.5	Drained
35N-200	35.0	0.59	200	0.54	51.1	Drained
35U-50	35.0	0.60	50	0.56	47.5	Undrained
25U-50	25.0	0.61	50	0.58	47.8	Undrained
15U-50	15.0	0.68	50	0.67	46.9	Undrained
0U-50	0.00	0.88	50	0.88	21.8	Undrained

Note: Specimens named with “E” means seepage tests have been performed on the specimens at a constant inflow rate of  $5.17 \times 10^{-6} \text{ m}^3/\text{s}$ , whereas those with “N” indicate the companion specimens without suffusion. Those specimens named with “U” are prepared for study of mechanical influence of fine fraction.

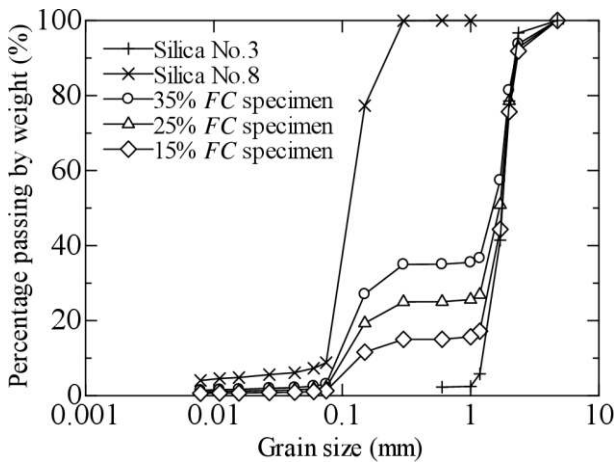
495

**Table 3** Summary of soil states after suffusion/before compression

Specimen	$i_{max}^{(1)}$	$k_i^{(2)}$ (m/s)	$k_e^{(3)}$ (m/s)	$FC^{(4)}$ (%)	$e_e/e_c^{(5)}$	$e_s^{(6)}$
35E-50	11.7	$9.7 \times 10^{-5}$	0.028	13.5	1.0	1.29
35E-100	7.17	$1.0 \times 10^{-4}$	0.010	15.9	0.92	1.29
35E-200	10.5	$1.0 \times 10^{-4}$	0.008	24.5	0.77	1.34
25E-50	5.05	$1.0 \times 10^{-4}$	0.009	12.0	0.81	1.06
15E-50	2.07	$1.2 \times 10^{-4}$	0.010	9.98	0.78	0.98
35N-50	---	---	---	35.0	0.55	1.39
35N-100	---	---	---	35.0	0.56	1.40
35N-200	---	---	---	35.0	0.54	1.37

Note: (1) Maximum hydraulic gradient,  $i_{max}$ ;  
 (2) Initial hydraulic conductivity before suffusion,  $k_i$  (m/s);  
 (3) Post-suffusion hydraulic conductivity,  $k_e$  (m/s);  
 (4) Fines content after suffusion/before compression for suffusional specimens and initial fines content for companion specimens,  $FC$  (%);  
 (5) Void ratio after suffusion/before compression for suffusional specimens,  $e_e$  and post-consolidation void ratio for companion specimens,  $e_c$ ;  
 (6) Intergranular void ratio  $e_s=(e_e+FC/100)/(1-FC/100)$  (suffusional specimens) and  $e_s=(e_c+FC/100)/(1-FC/100)$  (companion specimens).

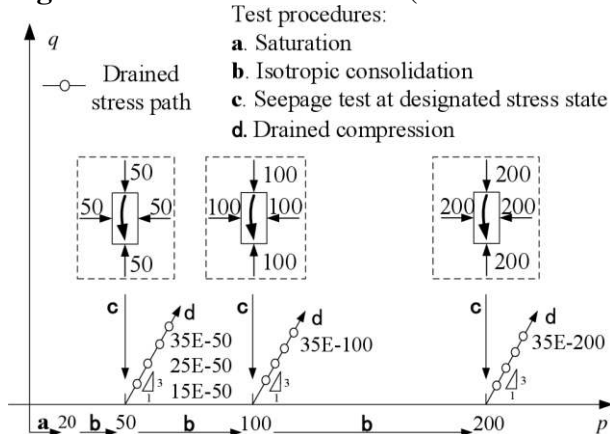
497



498

499

**Fig. 1.** Grain size distributions ( $FC$  indicates fines content)

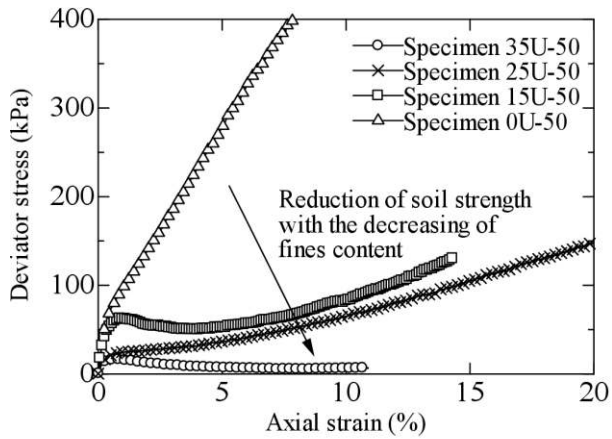


500

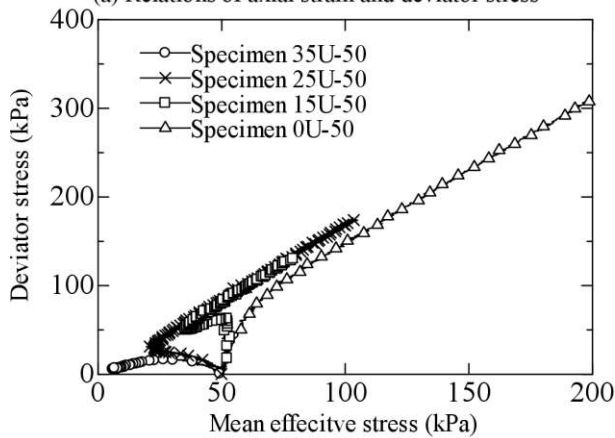
501

502

**Fig. 2.** Schematic diagram of test procedures in  $p'$ - $q$  space with test cases



(a) Relations of axial strain and deviator stress

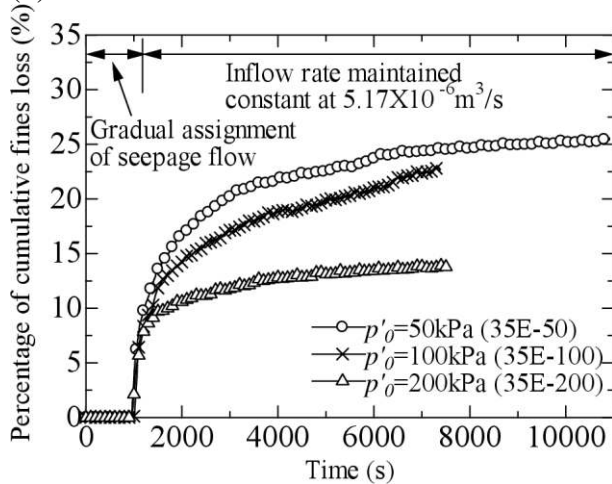


(b) Relations of mean effective stress and deviator stress

503  
504  
505  
506  
507

**Fig. 3.** Undrained compression tests on specimens with different contents of Silica No.8 under an initial effective confining pressure of 50kPa

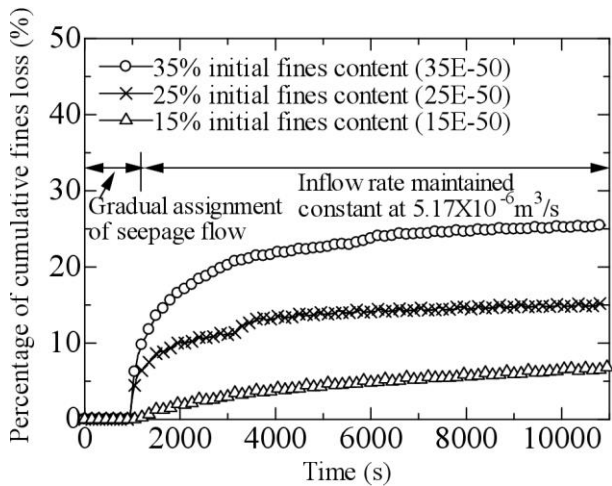
(a) Relations of axial strain and deviator stress  
(b) Relations of mean effective stress and deviator stress



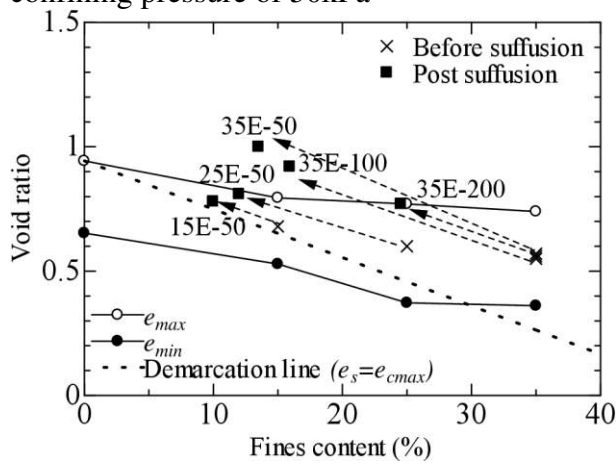
508  
509  
510

**Fig. 4.** Cumulative eroded soil mass with time for specimens with 35% initial fines content under different initial confining pressures

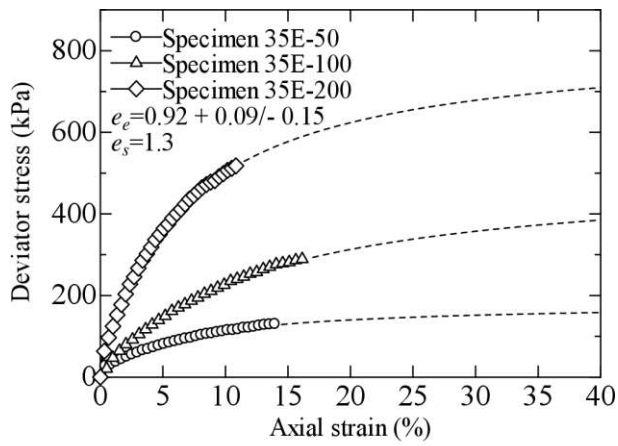




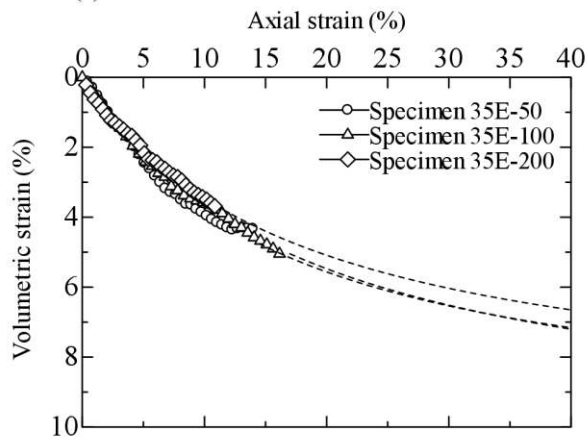
511  
512 **Fig. 5.** Cumulative eroded soil mass with time for specimens tested under an initial effective  
513 confining pressure of 50kPa



514  
515 **Fig. 6.** Changes of soil state induced by suffusion in fines content ~ void ratio space



(a) Relations of axial strain and deviator stress



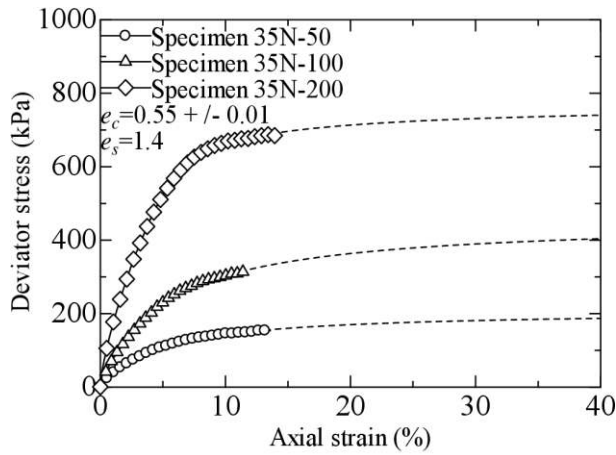
(b) Relations of axial strain and volumetric strain

516

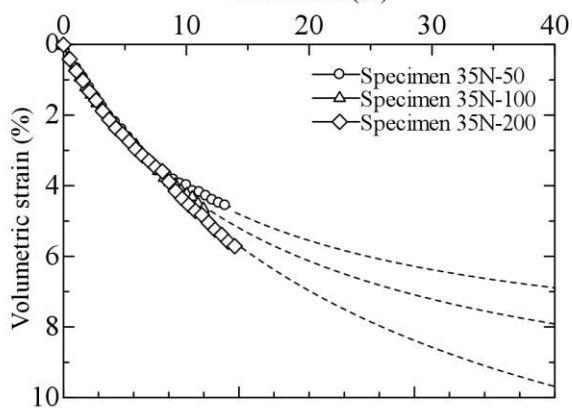
517 **Fig. 7.** Drained compression tests on suffusional specimens under different initial effective  
 518 confining pressures (Dash lines indicate the extrapolated curve by a hyperbolic fitting)

519 (a) Relations of axial strain and deviator stress

520 (b) Relations of axial strain and volumetric strain



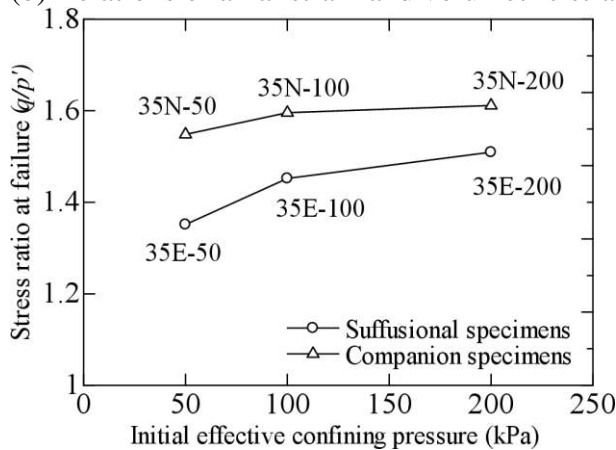
(a) Relations of axial strain and deviator stress



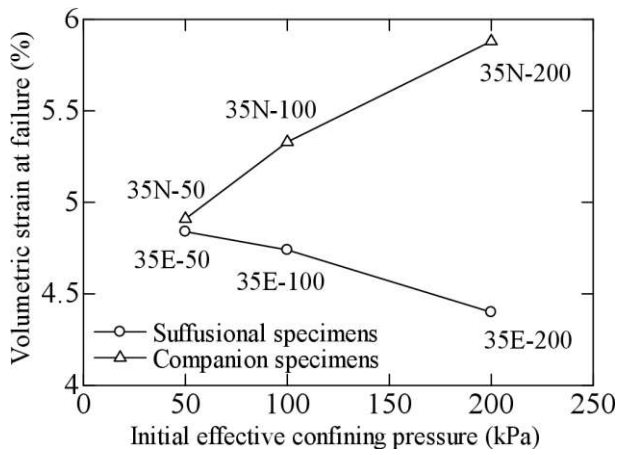
(b) Relations of axial strain and volumetric strain

521 **Fig. 8.** Drained compression tests on companion specimens under different initial effective  
 522 confining pressures (Dash lines indicate the extrapolated curve by a hyperbolic fitting)  
 523

524 (a) Relations of axial strain and deviator stress  
 525 (b) Relations of axial strain and volumetric strain

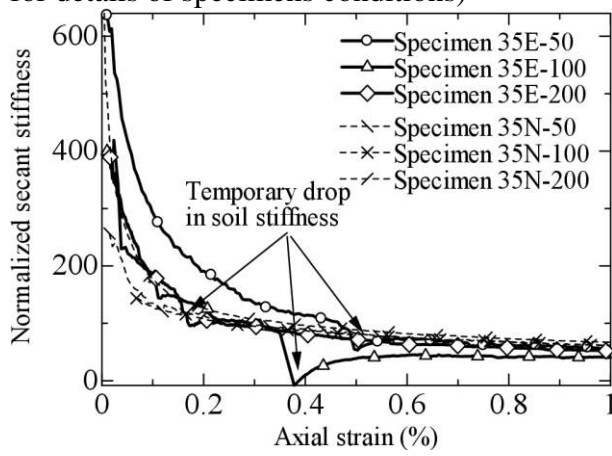


526 **Fig. 9.** Stress ratio at failure against initial effective confining pressure (refer Table 3 for  
 527 details of specimens conditions)  
 528



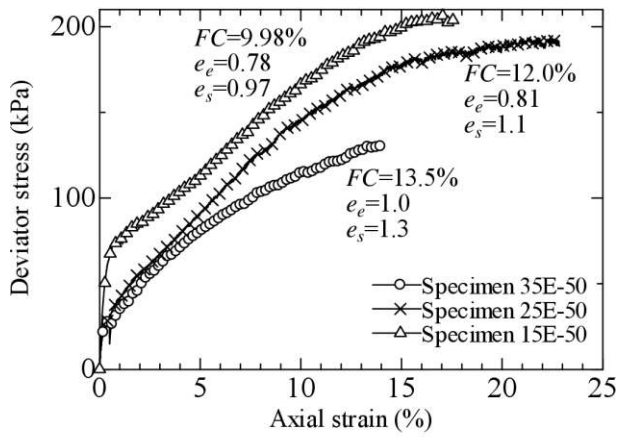
529  
530  
531

**Fig. 10.** Volumetric strain at failure against initial effective confining pressure (refer Table 3 for details of specimens conditions)

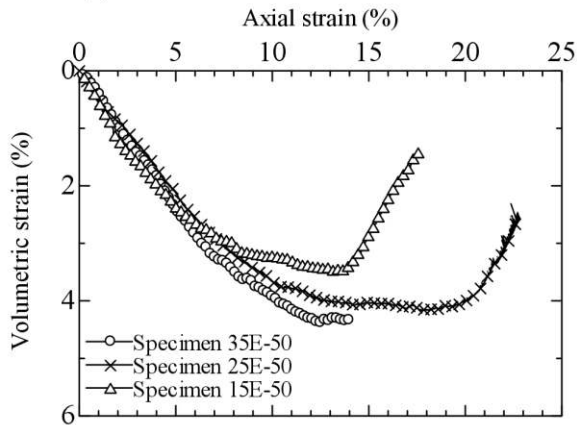


532  
533

**Fig. 11.** Normalized secant stiffness within 1% of axial strain



(a) Relations of axial strain and deviator stress



(b) Relations of axial strain and volumetric strain

534

535

536

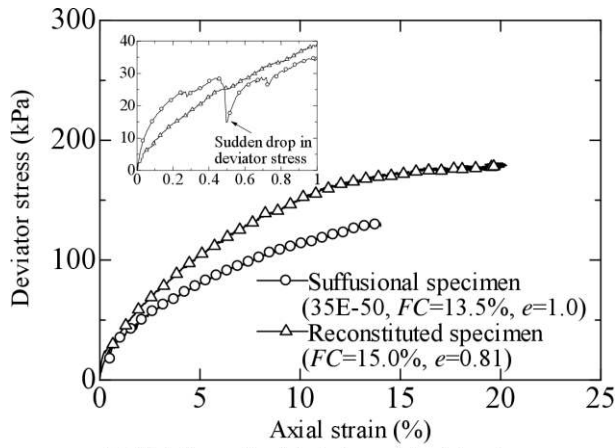
537

538

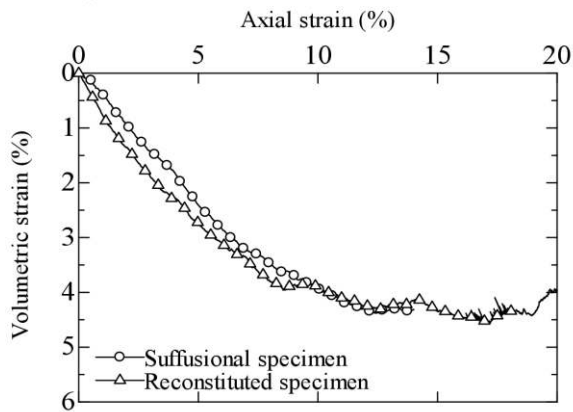
**Fig. 12.** Drained responses of suffusional specimens with different initial fines contents under an initial effective confining pressure of 50kPa

(a) Relations of axial strain and deviator stress

(b) Relations of axial strain and volumetric strain



(a) Relations of axial strain and deviator stress



(b) Relations of axial strain and volumetric strain

539  
540  
541  
542  
543  
544

**Fig. 13.** Drained responses of suffusional specimen and reconstituted specimen under an initial effective confining pressure of 50kPa

(a) Relations of axial strain and deviator stress  
(b) Relations of axial strain and volumetric strain